

## Manuscript Details

<b>Manuscript number</b>	IFSET_2017_1193_R1
<b>Title</b>	Innovative bioaerogel-like materials from fresh-cut salad waste via supercritical-CO <sub>2</sub> -drying
<b>Article type</b>	Research Paper

### Abstract

Fresh-cut salad waste was dried by means of supercritical carbon dioxide technology using ethanol as co-solvent. The obtained material was characterized by a white color and a brittle texture. Microscopic images revealed an aerated structure, with well-evident intra and inter-cellular spaces. Based on the high internal surface (>100 m<sup>2</sup>/g), the extremely low density (<0.5 g/cm<sup>3</sup>) and the high porosity (>80%), supercritical-dried salad waste can be regarded as a bioaerogel-like material. One gram of this material absorbed 33 and 19 g of water and oil respectively. Industrial application: Fresh-cut processing of salad generates large amounts of solid waste which is not suitable for conversion into biogas or fertilizers. This waste poses management issues for producers and represents an environmental burden. Fresh-cut salad waste could be valorized to produce bioaerogel-like materials with enhanced solvent uptake ability, to be exploited as food ingredients, packaging, absorbents or innovative carriers for both lipophilic and hydrophilic compounds.

<b>Keywords</b>	supercritical drying, salad waste, waste valorization, aerogel, porosity
<b>Corresponding Author</b>	Sonia Calligaris
<b>Corresponding Author's Institution</b>	University of Udine
<b>Order of Authors</b>	Stella Plazzotta, Sonia Calligaris, Lara Manzocco

## Submission Files Included in this PDF

### File Name [File Type]

Cover Letter.docx [Cover Letter]

Answers to the editors and reviewers.docx [Response to Reviewers]

Highlights.docx [Highlights]

Manuscript\_2nd subm.docx [Manuscript File]

Figures.docx [Figure]

Supplementary data.docx [Figure]

To view all the submission files, including those not included in the PDF, click on the manuscript title on your EVISE Homepage, then click 'Download zip file'.

Dear Editor,

We send to your attention the research article "**Innovative bioaerogel-like materials from fresh-cut salad waste via supercritical-CO<sub>2</sub>-drying**" by Stella Plazzotta, Sonia Calligaris and Lara Manzocco, revised according to the reviewers' suggestions and corrections.

Best regards,

Sonia Calligaris

## Answers to the editors and reviewers:

### Reviewer 1

This paper reports supercritical drying of salad waste and its absorption properties. I recommend the paper for publication after the following points are clarified:

1. On page 11, line 256, the authors pointed out that the high specific surface area of the aerogel compared to those of air dried samples is attributed to cell swallowing, or expansion, during drying. I don't think this speculation is correct because, i) In general, supercritically dried samples fundamentally show high specific surface areas compared to ambient dried samples because of the absence of surface tension during the drying process. ii) Simple expansion increases the volume of the sample, but it would not greatly affect internal surface areas. iii) You cannot simply compare the unit weights of air dried and supercritically dried samples. Supercritical drying also eliminates some CO<sub>2</sub>-soluble solids from the samples, e.g., pigments (page 10, line 235). See also comment 2 below.

i) We agree with the reviewer's observations that supercritical drying usually prevents sample collapse rather than promoting its expansions. This observation was added in the text (lines 309-313).

ii) Thank you for the observation. Mention to increase in sample area were omitted.

iii) The role of ethanol/CO<sub>2</sub> soluble compounds was discussed (lines 262-267, 318-321, 394-398).

2. On Page 13, line 314, the authors pointed out that the aerogel sample absorbs much water than fresh salad tissue because fresh salad contains 16 g water/1 g dry sample, while the aerogel absorbs ~35 g water/1 g dry sample. This item should be discussed more carefully. The fresh salad also contains some compounds that are removed via extraction with ethanol and/or supercritical CO<sub>2</sub>. The author should provide the chemical composition of the fresh salad: the ratio of water, CO<sub>2</sub>-insoluble components, and CO<sub>2</sub>-soluble components.

Discussion was improved by considering that removal of ethanol and CO<sub>2</sub> soluble compounds could favor exposure of hydrophilic groups and thus contribute to the development of a material able to uptake high amounts of water (lines 394-398). Composition of salad waste was added (lines 99-104, 258-267, Table 1) and the loss of compounds during the treatment, due to their solubility in both ethanol and CO<sub>2</sub> was discussed (lines 262-267, 318-321, 394-398).

3. The authors also pointed out that the CO<sub>2</sub>-dried sample has hydrophilic surface. In the case of silica aerogels, this is reasonable because supercritical-CO<sub>2</sub>-dried silica has strongly hydrophilic

surface due to the formation of Si-OH surface groups during the drying. In the present study, the authors should provide the experimental evidence for hydrophilicity and its origin, e.g., FT-IR, contact angle measurements.

The hygroscopicity and hydrophilicity of the material were evaluated (lines 181-198) and shown in two new supplementary figures (Supplementary Figure C and D). Additional considerations about material hydrophilicity were added in the text (lines 396-398).

4. The manuscript is well-organized and easy to follow. But, in my opinion, the authors should provide some raw data for the physicochemical properties described in Tables 1 and 2, e.g., stress-strain curves, DSC profiles, nitrogen isotherms, fitting curves, at least in the Supporting Information. Two supplementary figures relevant to material hygroscopicity and hydrophilicity were added in the supplementary data (Supplementary Figure C and D). Fitting was performed in a single step for the material isotherm and for oil and water absorption kinetics. Fitting curves were thus reported in Figure 2 and 3 and data in Table 4 were amended accordingly. In addition, stress-strain curves, nitrogen isotherms and a figure showing the appearance of the material after water imbibition were selected to be inserted in the paper supporting information (Supplementary Figure A and B).

5. The horizontal axis label in Figure 2 is not displayed properly.

The error was corrected.

## Reviewer 2

This manuscript presents an innovative idea of using salad waste to produce aerogels. The subject is clearly worthy of investigation, the applied characterization methods are appropriate, and the manuscript is generally well written. I suggest to consider the following points before the publication of this manuscript:

1) There seems to be a conflict between the BET surface area and pore size determination by optical microscopy, as those two methods may detect structures of different size ranges. The reported surface area would suggest a smaller pore size than that observed by microscopy. Were there pores in the mesoporous range that were not visualized by microscopy? Was the average pore size analyzed from the BET sorption results?

The discussion about porosity was modified, taking into account the reviewer's considerations. Actually BET and microscopy were able to detect different structures, that were distinctly discussed (lines 199-225, 300-307, 316-325, Table 3).

2) Please discuss the possibilities of manufacturing monoliths of various dimensions of the salad waste. Are the macroscopic dimensions of aerogels determined by the original dimensions of the salad leaves? How easy was it to cut the samples for e.g. mechanical testing and to obtain smooth surfaces?

This topic was discussed in the conclusions section (lines 429-432). Our material resulted brittle (according to stress-strain curves) but not difficult to cut.

3) Please report the possible shrinkage of the material upon ethanol treatment and drying

This topic was discussed in the text (lines 283-286).

4) Please discuss potential drawbacks of salad waste as raw material. The outer leaves remaining in the waste stream may be bruised and / or microbiologically spoiled. How does this affect the aerogel preparation and potential applications?

This topic was discussed in the conclusions section (lines 422-428).

### Reviewer 3

General:

The supercritical drying of cellular structures without necessary pretreatment (e.g. gel formation) is worth of investigation. Costly production steps of gel formation are not necessary and make it attractive. However, the technology is not new (Brown et al., 2007), but the performed analytics reveal new insights into the characteristics of such materials. Authors present the results of only one kind of sample (supercritically dried salad leaves) with one drying setup configuration. Hence the results of a single sample are presented. This leaves no possibility for comparison. The discussion of the present results is very short and a comparison to other materials presented in literature only takes place to a very limited extend.

We agree with the reviewer that the CO<sub>2</sub> drying is not new and has been proposed as alternative to freeze-drying to obtain high quality dried vegetable foods (see Brown et al., 2008). In our paper, we propose its exploitation to obtain food-grade materials which could be used to other purposes (e.g. moisture absorbents, templates for oleogels, biodegradable packaging). For this reason, the obtained material was characterized for physical and physico-chemical properties rather than for those properties which are usually assessed to evaluate dried food quality. This innovative approach

provided new insights in the material properties but reduces the possibility of comparison with literature results.

We decided to focus on salad waste, being representative of a number of plant waste materials, which are generally associated with management issues. As stated in the conclusions, it is likely that other waste materials could be similarly exploited.

Authors claim as industrial relevance that a valorization of the material is possible, but the technology is very expensive. Does the added value justify the process?

We agree with the reviewer about the high cost of the supercritical-drying technology. It can be hypothesized that turning a vegetable waste into a bio-aerogel like material with high loading solvent capacity would allow to reduce waste management issues as well as give a market value to the derived material. This topic was discussed in the conclusions section (lines 422-428). To assess the actual feasibility of this technology to salad waste, the evaluation of sustainability, economic and consumer impact of the obtained material should be investigated. Life Cycle Analysis could be exploited to this aim, which was however out of the scope of the present paper.

The discussion needs to be extended towards a clear hypothesis and description of how the existent structure, which is the obvious advantage of the material, will be transferred into an actual packaging, insulating or transportation material. Bioaerogels are gelled in the desired geometrical dimensions prior to supercritical drying. How is this intended with the described material?

Specific approaches should be adopted to provide the bioaerogel-like material with the desired shape, making it independent on the original dimension of the used vegetable waste. To this regard, the application to the ground vegetable waste of approaches commonly used to produce hydrogel and oleogel templates could be evaluated. More comments were added in the conclusion section (lines 428-432).

Providing that the authors have a clear prospect of how this is accomplished and they intensify the discussion, I recommend the manuscript for publication after major revision, since I clearly see the innovation and possible advantages of the subject.

Critical points in detail are:

**The article needs revision on spelling and wording. Examples are given in the following list.**

Line 126: Spelling Heerbrg

The mistake was corrected (lines 139-141).

Line 201, 232, 232, 261: Space missing

**Text was carefully controlled.**

Line 55: 'beget' is mainly used in a different context (beget a child).

**The term was changed in "produce" (line 50).**

Line 51: It is not clear whether the word 'process' refers to the solvent exchange or to the supercritical drying process.

**The term was changed in "supercritical-CO<sub>2</sub>-drying" (line 46).**

Line 271: 'controlled release in pharmaceuticals'

**The mistake was corrected (line 332).**

Line 103-105: The sentence is not clear. Reword. What is meant by visually assessed? This is very subjective.

**The sentence was reworded (lines 95-96).**

Line 137: Second sentence, wording.

**The mistake was corrected (line 143).**

Line 241, 251, 258: Wording. Do the authors mean swelling instead of swallowing? Reword 'peculiar swallowed'. Peculiar is more in the sense of unexplainable, which it is not, and swallowed is unclear. What is meant by 'cell swallowing'.

**The term was changed into "swelling" (lines 279-281).**

Line 330-332: Reword the sentence. It is hard to read.

**The sentence was reworded (lines 411-412)**

**Materials and Methods is in many cases not precise enough. Clarification is necessary in the following examples:**

Line 82: Point out more clearly that it is the outer leaves which are considered as salad waste and are the actual subject of investigation.

**The fact that outer leaves are considered as salad waste was better specified (lines 77-78).**

Line 84: Is the mass of the outer leaves of relevance for the investigated subject and where does a standard deviation come from? Was this registered per salad head? How is 'outer leaves' defined?

**Amount data was removed. As better explained in lines 76-78, salad heads were treated simulating industrial fresh-cut operations and thus outer leaves are those commonly removed during such operations.**

Line 85: Is the washing in a chlorinated bath with NaClO a standard process in the production process? Is it afterwards still applicable in food products? Authors promote the application in food products.

The washing in chlorinated water at 200 mg/L is a standard operation for fresh-cut products and thus the obtained material could still be used in food products.

Line 93: What was the final ethanol concentration in the surrounding solution? This has a major effect on the drying process. This question applies also to Line 98.

The concentration of the last ethanol solution was 99.04%, which, considering the alcoholmeter error, falls within the magnitude range of absolute ethanol concentration. For this reason, a complete substitution of compositional water by ethanol was assumed. Sentence was reworded (86-87).

Line 101: Explain the process in more detail. 5 g of sample, is this a stack of 5 cm x 5 cm pieces? Is it one piece?

Sample dimensions were reported more in detail (lines 82, 93, 202).

Line 107: Was a modification during storage monitored? P2O5 may initiate noteworthy drying of residual water, especially when water was not fully replaced by ethanol.

No change in sample weight was detected during storage up to 90 days.

Line 130: What about the BJH-method? This should deliver much more accurate results.

Both BET and microscopy were taken into consideration to discuss porous structure at different levels of size magnitude (lines 200-225, 300-307, 316-325).

Line 153: Were 5 mg of sample ground or cut?

Required information was added in line 158.

Line 165, 174, 188: Samples were described as very brittle. How was it possible to cut them in 2 x 2 cm squares? Where do differently sized samples come from. Original samples were cut in 5x5 cm. Outline more clearly the sample preparation and sample appearance.

Dimension units were harmonized and sample dimensions were reported more in detail in the different sections of material and methods (lines 82, 93, 202). Brittle materials break under a tensile stress without significant deformation (e.g a sheet of paper). This doesn't necessarily mean they are difficult to cut. Our material resulted brittle (according to stress-strain curves) but not difficult to cut.

Line 182: What was the cutting method used to obtain particles?

Required information was added in line 211.

Line 183: The drying temperature is very high. Did any changes occur on the sample? Was a further weight loss monitored (residual water)?

Required information was added in line 212-213. Such pre-treatments are reported in the literature for other vegetable matrices (Amin et al., 2015).

Line 190: Outline more clearly the function of the plastic filter.

Required information was added in line 229-230.

Line 213: How was it guaranteed that all pores were filled with oil? What about helium pycnometry?



As regards oil imbibition, we referred to a methodology previously reported in the literature by Khosravi & Azizian (2016). This methodology is based on the fact that, in a porous structure, small size pores are occupied by oil before the bigger ones. In the light of this interpretation, it can be inferred that pore size should not be a limiting factor for complete filling of the porous structure. Text was improved accordingly to these considerations (lines 301-302).

Line 219: Authors talk about 'two measurements'. Two equivalent measurements of the same sample should always deliver the same results. There is no added value. Furthermore, many methods may only be carried out once on one sample (Texture analyzer, DSC). Be more specific about how many experiments were carried out to attain reproducible results.

Two analytical repetition were performed on two replicated samples. Sentence was modified to increase clarity (lines 248-249).

### **Technology:**

Line 250: How was cutting of this brittle material possible for further analytics?

Tense tests revealed that the material was brittle. Nevertheless, it could be easily cut by simply using a sharp blade.

Line 262: Why is subsequent water removal necessary after supercritical drying? The process should be adjusted to producing samples without residual water.

Sentence was modified, as it was confounding and not clear. No residual water was present in the sample (lines 320-321).

Line 283: Figure 2: How was  $a_w$  0 and 100 accomplished? In Materials and Methods 11 and 96% are described as highest and lowest values for relative humidity.

Materials and methods were modified, adding information about 5 and 100% ERH (0.05-1  $a_w$ ) (lines 144-146). Figure 2 was modified accordingly.

Line 288: Authors claim that the samples did not lose their integrity. Were they still brittle and appeared dry or more like a wetted cloth?

The material appeared like a wetted cloth (lines 405-406). A clarifying image, showing sample appearance, was added in the supporting material (Supplementary Figure E).

### **Discussion:**

Line 234: (Figure 1) The L, a, b values do not supply valuable information to the reader, especially as the color change is obvious in the photographs. What meaningful information do the authors gain from the values?

It is our impression the complete loss of green color of the material is worthy mention. It accounts for porosity increase and removal of pigments. In addition, a white material could have larger possibilities of exploitation in several sectors.

Line 248: Specific heat is described as low, but compared to what? Discuss in more detail.

Sentence was rephrased, to underline that specific heat is simply comparable to that of similar dried vegetable matrices (lines 289).

Line 73: The poor composition of salad waste is mentioned. Why is it poor and what makes it then suitable for bioaerogel like materials? The composition is the same as in salad.

Table 1 was added, showing salad waste composition. Salad waste is actually not profitable for most recovery strategies as it is mainly represented by water and has low contents of bioactives as compared to other vegetable wastes. Text was improved (lines 66-68). Conversion to bioaerogel could allow exploitation of the salad structural architecture to obtain brand new materials.

Line 76: It would be helpful to outline the reasons for performing the analytics. What can be extracted and what is the new value.

Text was improved accordingly to the reviewer's suggestion (lines 70-72).

Line 253: Why is the brittle texture a reason for direct use in food systems. Discuss in more detail.

Most aerogels are very hard materials, difficult to cut and impossible to eat. The salad aerogel is brittle but not hard to cut or chew. This explanation was added in the text (lines 292-294).

Line 257: Is the advantage of CO<sub>2</sub>-drying not much more the retention of structure integrity but the ability to promote 'cell swallowing'?

We agree with the reviewer's comment and the sentence was thus modified (lines 309-313).

Line 267: The pore dimension is not discussed and is well above the typical pore dimension of aerogel materials, especially as it is out of the range of pores measurable using the BET method. The pores and therefore the surface measured using BET are mesopores and therefore in the range of 2 - 50 nm.

The discussion about porosity was modified. Both BET and microscopy were taken into consideration to discuss porous structure at different levels of size magnitude (lines 300-307, 316-325, Table 3).

Line 323: Mind the difference between loading efficiency and loading capacity. Ahmadi et al. (2016) had only about 2.5 % oil in their aerogels. They had a loading efficiency (% initially added to loaded on capsules) of 70 %.

The text was corrected (line 405).

Line 324: The oil holding capacity would be an interesting parameter. Is the oil kept inside or can the structure be described as a saturated sponge? The amount of oil makes it hard to imagine as dry brittle pellet with absorbed oil but rather a wet cloth containing large amounts of oil. In the latter case, the material would eventually be suitable as moisture absorbent but probably not as carrier system. Discuss in more detail.

Thank you for the advice. Text was improved accordingly (line 406-408).

Line 337: Low firmness and brittleness do not really qualify the material for further production steps as for example storage or transportation. Is it really possible to further process the dried material? Discuss in more detail.

Proper storage and packaging techniques should be defined once the commercial value of the material is proven. If this was true, packaging and transport solutions similar to those adopted for other brittle materials (dried pasta, eggs, bulbs, ...) could be adopted. Conclusion section was improved, by adding considerations about the possible issues related to the conversion of vegetable wastes into bioaerogel-like materials by supercritical drying (lines 422-432).

- 1 Porous materials can be obtained by supercritical-drying of vegetable wastes
- 2 Supercritical-CO<sub>2</sub>-dried salad waste can be regarded as a bioaerogel-like material
- 3 Mechanical properties of dried salad waste would allow its use in food systems
- 4 Dried salad waste presented extremely high solvent loading capacity
- 5 Bioaerogel-like materials could be exploited as adsorbents and carriers

1 **Innovative bioaerogel-like materials from fresh-cut salad waste**

2 **via supercritical-CO<sub>2</sub>-drying**

3 Plazzotta, S., Calligaris, S.\*, Manzocco, L.

4 Department of Agricultural, Food, Environmental and Animal Sciences, University of Udine,

5 Italy

6 \*e-mail: [sonia.calligaris@uniud.it](mailto:sonia.calligaris@uniud.it); Tel: +39 0432-558571

7 **Abstract**

8 Fresh-cut salad waste was dried by means of supercritical carbon dioxide technology using  
9 ethanol as co-solvent. The obtained material was characterized by a white color and a brittle  
10 texture. Microscopic images revealed an aerated structure, with well-evident intra and inter-  
11 cellular spaces. Based on the high internal surface ( $>100 \text{ m}^2/\text{g}$ ), the extremely low density ( $<0.5$   
12  $\text{g}/\text{cm}^3$ ) and the high porosity ( $>80\%$ ), supercritical-dried salad waste can be regarded as a  
13 bioaerogel-like material. One gram of this material absorbed 33 and 19 g of water and oil  
14 respectively.

15 *Industrial application:* Fresh-cut processing of salad generates large amounts of solid waste  
16 which is not suitable for conversion into biogas or fertilizers. This waste poses management  
17 issues for producers and represents an environmental burden. Fresh-cut salad waste could be  
18 valorized to produce bioaerogel-like materials with enhanced solvent uptake ability, to be  
19 exploited as food ingredients, packaging, absorbents or innovative carriers for both lipophilic  
20 and hydrophilic compounds.

21 **Keywords:** supercritical drying, salad waste, waste valorization, aerogel, porosity

22 **1 Introduction**

23 Aerogels are defined as microporous materials entrapping a gas phase within the pores (Jones,  
24 2007). The term is generic and refers to a wide variety of materials, presenting low density  
25 ( $0.0003\text{-}0.5 \text{ g}/\text{cm}^3$ ), high surface area ( $50\text{-}1200 \text{ m}^2/\text{g}$ ) and high porosity ( $70.0\text{-}99.8\%$ ) (Fricke  
26 & Tillotson, 1997). Based on their composition, aerogels can be classified into inorganic,

27 organic, hybrid and bioaerogels. Although studies about bioaerogels are still pioneering, they  
28 have raised great interest in the last years, being produced from natural sources such as cellulose  
29 and its derivatives, marine polysaccharides, starch and proteins (Stergar & Maver, 2016).  
30 Bioaerogels are biocompatible, biodegradable and food-grade, making them potentially  
31 applicable in medical engineering, sustainable packaging production and novel food  
32 development (Maleki, 2016). To this regard, bioaerogels were proposed as carriers for different  
33 solvents, due to their ability to absorb large amounts of liquids by capillary forces (Ahmadi,  
34 Madadlou, & Saboury, 2016; Comin, Temelli, & Saldaña, 2012; Ivanovic, Milovanovic, &  
35 Zizovic, 2016). In this context, they have been suggested as food bulking agents, templates for  
36 liquid oil structuring and innovative carriers of nano-sized biochemicals (Ahmadi et al., 2016;  
37 Manzocco et al., 2017; Ubeyitogullari & Ciftci, 2017).

38 To obtain bioaerogels, a two-step procedure is traditionally applied. Initially, hydrogels are  
39 produced by gelation of a biopolymer in an aqueous media. Following, hydrogel solvent is  
40 slowly removed by a flow of continuous supercritical-CO<sub>2</sub>. The latter is commonly applied  
41 since it avoids the formation of liquid-vapor interfaces and capillary tensions, thus reducing  
42 local collapse and maintaining the original hydrogel network (Maleki, 2016). The time required  
43 for supercritical-CO<sub>2</sub>-drying is generally reduced by an ethanol-assisted procedure. In this case,  
44 before drying, hydrogel aqueous phase is substituted with ethanol, which has a higher affinity  
45 to supercritical-CO<sub>2</sub> (García-González, Camino-Rey, Alnaief, Zetzl, & Smirnova, 2012;  
46 Viganó, Machado, & Martínez, 2015). **Supercritical-CO<sub>2</sub>-drying** is regarded as sustainable  
47 since it is performed at mild pressure (<10 MPa) and temperature (<45 °C), often using recycled  
48 carbon dioxide (Ghafar et al., 2017).

49 It can be inferred that supercritical-CO<sub>2</sub>-drying of biological systems other than biopolymer  
50 gels could also **produce** highly aerated structure, similar to that of bio-aerogels. For instance,  
51 moisture-rich plant tissues could represent optimal candidates for the preparation of bioaerogel-  
52 like materials. These vegetable matrices can be regarded as complex polymeric networks,

53 mainly structured by cell wall cellulosic fibers, embedding water within intra- and inter-cellular  
54 spaces. Water removal, while maintaining cellular organization, could possibly result in an  
55 aerated fibrous network with high internal surface area and porosity. Circumstantial evidence  
56 supporting this hypothesis could be the enhanced rehydration ability of fruit and vegetables  
57 submitted to supercritical-CO<sub>2</sub>-drying (Brown, Fryer, Norton, Bakalis, & Bridson, 2008).  
58 The preparation of bioaerogel-like materials from vegetable tissues could present the advantage  
59 of simplifying the conventional production process, since not requiring the gelling phase. In  
60 addition, if applied to vegetable wastes, this technological strategy could allow valorization of  
61 industrial discards, which typically represent an environmental and economic burden (Raak,  
62 Symmank, Zahn, Aschemann-Witzel, & Rohm, 2017).  
63 Based on these considerations, the aim of the present study was to evaluate the possibility to  
64 exploit salad waste to produce bioaerogel-like materials by means of supercritical-CO<sub>2</sub>-drying.  
65 Fresh-cut salad was chosen as an example of a vegetable waste with high water content, which  
66 is not profitable for conventional valorization strategies (e.g. biogas production, composting or  
67 bioactive extraction) due to its poor composition, that is mainly represented by water (>94%  
68 w/w) (Plazzotta, Manzocco, & Nicoli, 2017). Salad waste was submitted to ethanol solvent  
69 exchange and supercritical-CO<sub>2</sub>-drying. Samples were then analyzed for optical, thermal,  
70 mechanical and structural properties as well as for the ability to uptake water and oil. Analyses  
71 were performed in order to get an insight in the physical and physico-chemical properties of the  
72 material to suggest possible applications.

## 73 2 Materials and methods

### 74 2.1 Vegetable material

75 A 10-kg batch of Iceberg salad (*Lactuca sativa* var. *capitata*) was purchased at the local market  
76 and stored overnight at 4 °C. Salad head were treated simulating operations that are industrially  
77 carried out during fresh-cut salad processing. In particular, outer leaves were removed and used  
78 for the experimentation. Leaves were washed with flowing water (18±1 °C) and sanitized 20

79 min in a chlorinated bath containing 200 mg/L of NaClO with a 100 g/L leaves/water ratio.  
80 Leaves were then rinsed with flowing water and centrifuged in a manual kitchen centrifuge  
81 (mod. ACX01, Moulinex, France) for 1 min. Salad waste was manually chopped in  
82 homogeneous pieces (about  $2.5 \times 5$  cm) with a sharp knife and immediately submitted to solvent  
83 exchange.

#### 84 2.2 *Solvent exchange using ethanol*

85 Salad waste was immersed (100 g/L) in pure ethanol (J.T. Baker, Centre Valley, USA) for 24  
86 h twice. During this procedure, water was progressively and completely removed from salad  
87 leaves, as indicated by monitoring the alcoholic degree of the ethanol solution by a lab  
88 alcoholmeter (Alcolyzer plus, Anton Paar, Graz, Austria).

#### 89 2.3 *Supercritical-CO<sub>2</sub>-drying*

90 Salad waste in which water had been substituted by ethanol was dried using a supercritical-  
91 CO<sub>2</sub>-drying plant developed at the Department of Agricultural, Food, Environmental and  
92 Animal Sciences of the University of Udine and previously described by Manzocco et al.  
93 (2017). Briefly, a salad piece of  $2.5 \times 5.0$  cm was placed inside the 265 mL-volume stainless  
94 steel cylindrical reactor which was then pressurized with CO<sub>2</sub> at  $11 \pm 1$  MPa and 45 °C. The  
95 outlet flow through the reactor was set at 6.0 L/min. This flow value was selected since it  
96 allowed drying time to be minimized. Samples were considered dried when ethanol was no  
97 more detectable in the gaseous outlet. Decompression from 11 MPa to atmospheric pressure  
98 was then carried out in 30 min. Samples were stored in P<sub>2</sub>O<sub>5</sub> at room temperature until use.

#### 99 2.4 *Salad waste composition*

100 Moisture, ash, protein and fat content was calculated according to AOAC methods (AOAC,  
101 1997). Total dietary fibre (TDF) was calculated according to the AOAC international method  
102 (AOAC, 1997) using a total dietary fibre assay kit (TDF – 100A, Sigma-Aldrich, St. Louis,  
103 Missouri, USA). Carbohydrates were calculated by difference from moisture, ash, fat, protein  
104 and TDF.



#### 2.4.1 *Total polyphenolic content*

An amount 10 g of salad waste, trimmed with a sharp knife were extracted by reflux with boiling water for 60 min applying a dilution of 1:4 (w/v). Extracts were cooled at room temperature, vacuum filtered thorough Whatman no. 1 filter paper (Maidstone, UK), freeze-dried at -50 °C and stored in a desiccator containing P<sub>2</sub>O<sub>5</sub> at room temperature until use. Total polyphenolic content (TPC) was determined using Folin-Ciocalteu reagent (Singleton & Rossi, 1985). The reaction mixture contained 100 µL of salad waste extract solubilised in water (1:10 w/v), 500 µL of the Folin-Ciocalteu reagent, 4 mL of water and 2 mL of a sodium carbonate-water solution (0.15 g/mL). After 2 h reaction at ambient temperature, mixture absorbance was read at 750 nm using US-Vis spectrophotometer (Shimadzu UV-2501PC, UV-Vis recording spectrophotometer, Shimadzu Corporation, Kyoto, Japan). A calibration curve was made with standard solutions of gallic acid in the range 0.1–1000 mg/L (R<sup>2</sup>=0.99). Results were expressed as mg of gallic acid equivalents per g of dry weight.

#### 2.4.2 *Chlorophyll content*

Salad waste was homogenized with ethanol (95% w/w) applying a dilution of 1:4 (w/v) and filtered. The chlorophyll content was determined spectrophotometrically (Shimadzu UV-2501PC, UV-Vis recording spectrophotometer, Shimadzu Corporation, Kyoto, Japan), using the Lambert-Beer law and the specific absorbance coefficient ( $\alpha$ ) for chlorophyll  $\alpha$  in 95% ethanol (84.6 Lg<sup>-1</sup>cm<sup>-1</sup>) (Lichtenthaler & Buschmann, 2001; Perucka, Olszówka, & Chilczuk, 2014). Results were expressed as µg of chlorophyll per mg of dry weight.

#### 2.5 *Color*

Color determination was carried out on salad waste using a tristimulus colorimeter (Chromameter-2 Reflectance, Minolta, Osaka, Japan) equipped with a CR-300 measuring head. The instrument was standardized against a white tile before measurements. Color was expressed in L\*, a\* and b\* Hunter scale parameters (Chen, Zhu, Zhang, Niu, & Du, 2010).

#### 2.6 *Image acquisition*

131 Images were acquired using an image acquisition cabinet (Immagini & Computer, Bareggio,  
132 Italy) equipped with a digital camera (EOS 550D, Canon, Milano, Italy). The digital camera  
133 was placed on an adjustable stand positioned 45 cm above a black cardboard base where the  
134 samples were placed. Light was provided by 4 100 W frosted photographic floodlights, in a  
135 position allowing minimum shadow and glare. Images were saved in *jpeg* format resulting in  
136 3456 x 2304 pixels.

### 137 2.7 *Optical microscopy*

138 Samples were observed at room temperature using a Leica DM 2000 optical microscope (Leica  
139 Microsystems, Heerbrugg, Switzerland). The images were taken at 200X magnification using  
140 a Leica EC3 digital camera (Leica Microsystems, Heerbrugg, Switzerland) and elaborated with  
141 the Leica Suite Las EZ software (Leica Microsystems, Heerbrugg, Switzerland).

### 142 2.8 *Sorption isotherm*

143 Samples were weighted and transferred into dried weighting bottles. The latter were then  
144 transferred into desiccators containing P<sub>2</sub>O<sub>5</sub> and LiCl, CH<sub>3</sub>COOK, CaCl<sub>2</sub>, K<sub>2</sub>CO<sub>3</sub>, NaCl, KCl,  
145 K<sub>2</sub>SO<sub>4</sub> saturated solutions and water with equilibrium relative humidity (ERH%) values of 5,  
146 11, 25, 31, 43, 75, 86, 96 and 100%, respectively. Samples were kept inside desiccators until  
147 constant weight was reached. The Brunauer-Emmet-Teller (BET) sorption isotherm model (eq.  
148 1) was fitted into water sorption data (Braunauer, Emmett, & Teller, 1938).

$$149 \frac{a_w}{m(1-a_w)} = \frac{1}{m_0c} + \frac{c-1}{m_0c} a_w \quad (1)$$

150 where  $a_w$  is the water activity,  $m$  is the moisture of the sample expressed as ratio between the  
151 weight (g) of absorbed water and the weight (g) of dry matter,  $m_0$  is the moisture of the water  
152 monolayer, and  $c$  is an experimental constant.

### 153 2.9 *Differential Scanning Calorimetry (DSC)*

154 DSC analysis was carried out using a TA4000 differential scanning calorimeter (Mettler-  
155 Toledo, Greifensee, Swiss) connected to a Graph Ware software TAT72.2/5 (Mettler-Toledo).

156 Heat flow calibration was achieved using indium (heat of fusion 28.45 J/g). Temperature  
157 calibration was carried out using hexane (m.p. -93.5 °C), water (m.p. 0.0 °C) and indium (m.p.  
158 156.6 °C). Samples were prepared by carefully weighing around 5 mg of **cut** sample in 160 µL  
159 aluminum DSC pans, closed with hermetic sealing. An empty pan was used as a reference in  
160 the DSC cell.

161 For determination of specific heat capacity ( $C_p$ , Jg<sup>-1</sup>K<sup>-1</sup>), dried salad waste was heated from 15  
162 to 150 °C, at a constant heating rate of 10 °C/min and without purge gas. A blank curve was  
163 also recorded by submitting an empty sealed pan to the same analysis.  $C_p$  (40 °C) was  
164 determined according to the following eq. (2):

$$165 \quad C_p = \frac{H}{r_T} \cdot \frac{1}{m} \quad (2)$$

166 Where  $H$  is the heat flow in mW, calculated as signal difference between sample and blank  
167 curve,  $r_T$  is the sample heating rate (K/s) and  $m$  is the sample mass in mg.

#### 168 2.10 Specific volume and apparent density

169 Samples were cut into 2 × 2 cm square shape and accurately weighted. Sample volume was  
170 then measured by a CD-15APXR digital caliber (Absolute AOS Digimatic, Mitutoyo  
171 Corporation, Kanagawa, Japan) and expressed as specific volume (cm<sup>3</sup>/g). Sample apparent  
172 density (g/cm<sup>3</sup>) was then calculated as the ratio between sample weight and specific volume.

#### 173 2.11 Mechanical properties

174 Sample mechanical properties were measured by uniaxial tensile test using an Instron 4301  
175 (Instron LTD., High Wycombe, UK). The instrumental settings and operations were  
176 accomplished using the software Automated Materials Testing System (version 5, Series IX,  
177 Instron LTD., High Wycombe, UK). Rectangular samples (2 × 4 cm) were positioned between  
178 two clamps mounted on a 100 N tensile head at a 5 mm/min crosshead speed, with a gauge  
179 length of 1 cm. Stress-strain curves were obtained from the tensile tests. Tensile strength at  
180 break (N) and the elongation at break (mm) were used to characterize sample tensile strength.

## 181 2.12 Hygroscopicity

182 The hygroscopicity was determined by measuring the moisture absorption capacity of samples  
183 at a set relative humidity (RH) of 86% at 30 °C. For this purpose, saturated solution of  
184 potassium chloride (KCl) was used. Samples were kept in desiccators with the set RH and  
185 weighed over time until a constant weight was reached. The percentage of moisture sorption  
186 (*MS*) was calculated from eq. (3):

$$187 \quad MS = \frac{W - W_0}{W_0} \times 100 \quad \text{eq. (3)}$$

188 where, *W* (g), and *W*<sub>0</sub> (g) are the material weight after moisture sorption and its initial weight,  
189 respectively (Su et al., 2010).

## 190 2.13 FTIR measurement

191 Spectra were recorded at 25 ± 1 °C using a FTIR instrument, equipped with a ATR accessory  
192 and a Zn-Se crystal that allows collection of FTIR spectra directly on sample without any  
193 special preparation (Alpha-P, Bruker Optics, Milan, Italy). The “pressure arm” of the  
194 instrument was used to apply constant pressure to the samples positioned on the top of the Zn-  
195 Se crystal, to ensure a good contact between the sample and the incident IR beam. All FTIR  
196 spectra were collected in the range from 4000 to 400 cm<sup>-1</sup>, at a spectrum resolution of 4 cm<sup>-1</sup>  
197 and with 32 co-added scans. Background scan of the clean Zn-Se crystal was acquired prior to  
198 sample scanning.

## 199 2.14 Porosity

### 200 2.14.1 Total pores

201 Oil imbibition was exploited for total porosity determination (Khosravi & Azizian, 2016).  
202 Samples (2 × 2 cm square shape) were immersed into oil until constant weight, as described in  
203 section 2.14. Based on oil density (0.89 g/cm<sup>3</sup>), the oil volume absorbed by samples was  
204 calculated and used to estimate total porosity (%). In particular, the latter was calculated as the

205 ratio between the volume of the absorbed oil and sample specific volume determined as  
206 described in section 2.10.

#### 207 2.14.2 Mesoporous structures

208 A gas analyzer was employed with nitrogen gas at -196 °C to investigate sample mesoporous  
209 structures, i.e. pore diameter, pore volume and specific surface area. The latter were determined  
210 based on Brunauer-Emmett-Teller (BET) model (Braunauer, Emmett, & Teller, 1938). Samples  
211 were cut using a sharp scissors and sieved to obtain particles in the range 1-2 mm, and dried at  
212 110 °C for 2 h in an oven (UM100, Memmert, Schwabach, Germany). No significant changes  
213 in sample weight was detected upon this pre-treatment. Then, about 10 mg of sample, accurately  
214 weighted, was placed inside the analyzer. Pore diameter, pore volume and specific surface area  
215 of 1 g-sample were obtained after 24 h. The ratio % between mesopore total volume and total  
216 pore volume, determined as described in paragraph 2.14.1, was used to determined mesopore  
217 total volume ratio. The latter was defined as the contribution of mesopores to sample total pore  
218 volume.

#### 219 2.14.3 Macroporous structures

220 Pore dimension was estimated based on image analysis of optical microscopic images by using  
221 Image-Pro® Plus (ver. 6.3, Media Cybernetics, Inc., Bethesda, MD, USA). Images were  
222 divided into 8 sections and the longitudinal radius ( $\mu\text{m}$ ) of 10 pores present in each section were  
223 measured by comparison with a 50  $\mu\text{m}$  scale. Total macropore volume and macropore total  
224 volume ratio were estimated by the difference between data relevant to total pores and  
225 mesopores.

#### 226 2.15 Water and oil absorption kinetics

227 Samples of  $2 \times 2$  cm square shape were introduced into 50 mL beakers previously filled with  
228 15 mL of water or sunflower oil and maintained at room temperature. The complete immersion  
229 of samples in the liquid phase was assured by using a plastic filter, preventing sample from  
230 floating. At defined time intervals, samples were withdrawn, wiped with absorbing paper and

231 weighted. Absorbed water or oil was expressed as the ratio between weight gain at time  $t$  and  
232 the initial weight of the dried sample. The immersion of sample into water or oil was prolonged  
233 until a constant weight after three consequent readings was reached.

234 Absorption kinetic data were then elaborated by fitting a two-phase exponential decay model  
235 (eq. 4) (Blake, Co, & Marangoni, 2014).

$$236 \quad y = y_{fast}(1 - e^{(-k_{fast}t)}) + y_{slow}(1 - e^{(-k_{slow}t)}) \quad (4)$$

$$237 \quad y_{max} = y_{fast} + y_{slow} \quad (5)$$

238 where  $y_{fast}$  and  $y_{slow}$  are the asymptote values of the fast- and slow-decaying components,  
239 respectively,  $k_{fast}$  and  $k_{slow}$  are the rate constants for the fast- and slow-decaying component,  
240 respectively, and  $y_{max}$  is the maximum amount of absorbed water or oil when time  $t$  tends to  
241 infinite and is the sum of  $y_{fast}$  and  $y_{slow}$  (eq. 5). The value  $y_{max}$  can also be considered the  
242 theoretical *plateau* value.

#### 243 2.16 Water and oil absorption capacity

244 Water and oil absorbing capacities of dried leaves were calculated from water and oil absorption  
245 data (Section 2.14), as the amount of water or oil (g) present in 1 g of sample at the absorption  
246 *plateau* value ( $y_{max}$ ).

#### 247 2.17 Data analysis

248 All determinations were expressed as the mean  $\pm$  standard error of at least two repeated  
249 measurements from two experiment replicates ( $n \geq 4$ ). Statistical analysis was performed by  
250 using R v. 3.0.2 (The R foundation for Statistical Computing). Student's t-test was used to  
251 determine statistical significant differences among means ( $p < 0.05$ ). Non-linear regression  
252 analysis of absorbed water and oil as a function of sample mass was performed by using  
253 TableCurve2D software (Jandel Scientific, ver. 5.01). Levenberg-Marquardt algorithm was  
254 used to perform least squares function minimization and the goodness of fit was evaluated based  
255 on statistical parameters of fitting ( $R^2$ ,  $p$ , standard error) and the residual analysis.

## 257 3 Results and discussion

### 258 3.1 Characterization of salad waste

259 Salad waste composition was determined, as shown in Table 1, to highlight the presence of  
260 ethanol CO<sub>2</sub>-soluble compounds, which, along with water, are expected to be lost upon  
261 supercritical-CO<sub>2</sub>-drying  
262 Beside water, other compounds such as fat, polyphenols and chlorophylls can be easily  
263 dissolved during the supercritical-CO<sub>2</sub> treatment (Fiori, de Faveri, Casazza, & Perego, 2009;  
264 Guedes et al., 2013; Lan, Wu, Zhang, Hu, & Liu, 2011; Roy, Goto, Kodama, & Hirose, 1996).  
265 These compounds represented about 3.87% of salad waste dry weight. This suggests that the  
266 change in salad waste properties upon supercritical-CO<sub>2</sub>-drying should be attributed not only to  
267 water removal but also to the loss of these compounds.

### 268 3.2 Characterization of supercritical-CO<sub>2</sub>-dried salad waste

269 Waste external leaves from fresh-cut Iceberg salad processing were submitted to supercritical-  
270 CO<sub>2</sub>-drying after substituting compositional water with ethanol. Figure 1 shows the effect of  
271 this procedure on visual appearance, color and microscopic structure of salad waste.  
272 Dried salad waste completely lost the original green color. Red point significantly increased  
273 while yellow point decreased. This can be attributed to tissue bleaching upon pigment extraction  
274 from salad leaves during immersion into ethanol. An increase in luminosity (L\*) was also  
275 observed (Figure 1), probably due to an increase in light scattering phenomena, generally  
276 associated to materials with a high surface roughness (Krokida, Maroulis, & Saravacos, 2001).  
277 The micrographs (Figure 1) showed that fresh tissue cells were regular in shape and appeared  
278 turgid with well-defined cell wall structure. Stoma leaf cells were also evident. Supercritical-  
279 CO<sub>2</sub>-drying did not affect cell integrity but promoted cell swelling as well as the increase of  
280 intercellular space. It is likely that cell expansion occurred during the decompression phase,  
281 which is required to remove pressurized CO<sub>2</sub> from the sample after drying. Swelling phenomena  
282 upon supercritical-CO<sub>2</sub>-drying has also been reported for other vegetable matrices, such as

283 carrot (Brown et al., 2008). By contrast, most bioaerogels have been reported to undergo severe  
284 shrinkage upon both ethanol substitution and supercritical-CO<sub>2</sub>-drying, as a result of the  
285 different structural organization of the gel network depending on the solvent nature  
286 (Therkelsen, 1993).

287 To investigate the physico-chemical characteristics of the material obtained by supercritical-  
288 CO<sub>2</sub>-drying of salad waste, its thermal and mechanical properties were analyzed (Table 2).  
289 Specific heat of the sample resulted in the same range of that reported in the literature for other  
290 dried vegetable materials (Mykhailyk & Lebovka, 2013). Based on stress-strain diagrams  
291 (Supplementary Figure A), CO<sub>2</sub>-dried salad waste resulted a brittle material, presenting low  
292 values of tensile strength and deformation at break. This can be regarded as a positive attribute  
293 of the material, since, differently from other food-grade bioaerogels (Manzocco et al., 2017), it  
294 is not hard and could be thus directly used in food systems. To better characterize the properties  
295 of this material, apparent density was evaluated, resulting in a very low value, corresponding  
296 to a high specific volume (Table 2). These properties suggest that a light weighted and porous  
297 material was obtained upon supercritical drying. Total sample porosity was thus evaluated  
298 exploiting oil imbibition technique (Khosravi & Azizian, 2016). According to the latter, oil  
299 absorption into porous materials such as synthetic aerogels leads firstly to the imbibition of  
300 smaller-size pores and then to the imbibition of larger ones, until reaching a *plateau*. It is thus  
301 likely that the latter value can be used to estimate total pore volume. Total pore volume and  
302 porosity of the material obtained by supercritical-CO<sub>2</sub>-drying of salad waste is reported in Table  
303 3. To get an insight into the porous structures of the obtained material, BET analysis, which is  
304 conventionally applied to analyze mesopore surface, volume and dimension was also exploited  
305 (Wiman et al., 2012) (Table 3). Supplementary Figure B reports an example of the nitrogen  
306 isotherms obtained by BET analysis. The latter revealed the presence of mesoporous structures  
307 presenting an average dimension of 47 nm. As expected, the value of internal surface area  
308 resulted much higher than that reported by Amin, Abkenar, & Zendehboudi (2015), for an air-



309 dried water fern intended for oil spill absorption (4.7 m<sup>2</sup>/g). This difference is attributable to  
310 the capacity of supercritical-CO<sub>2</sub>-drying to hinder structural collapse, due to the absence of  
311 surface tension during the drying treatment (Michalska, Wojdyło, Lech, Łysiak, & Figiel,  
312 2017). Moreover, it can also be due to the cellular structure swelling clearly observed in  
313 microscopic images (Figure 1). Interestingly, sample internal surface area resulted in the same  
314 range of that reported by Ghafar et al. (2017) and Ubeyitogullari & Ciftci (2017) for aerogels  
315 obtained via supercritical-CO<sub>2</sub>-drying of hydrogels containing different biopolymers such as  
316 guar galactomannan (99-333 m<sup>2</sup>/g) and nanoporous starch (60-63 m<sup>2</sup>/g). It is noteworthy that  
317 mesopores detected by BET analysis presented an average total volume pore of about 2.8 cm<sup>3</sup>/g,  
318 contributing to the total sample pore volume by only 11%. Based on these observations, it is  
319 likely that most pores in the sample were not accounted for by these mesopores but rather by  
320 larger macropores, corresponding to cellular voids left upon removal of water and other  
321 compounds that are soluble in ethanol or CO<sub>2</sub>. These cellular voids were not detectable by BET  
322 technique but clearly observed in photomicrographs (Figure 1). The latter actually showed these  
323 cell voids to present dimensions much higher than those estimated for mesopores by BET  
324 technique (Table 3). Based on this hypothesis, 89% of the sample pore volume, corresponding  
325 to a value of about 22.8 cm<sup>3</sup>/g, was developed by macropores (Table 3).

326 It is noteworthy that the obtained values of internal surface area and total porosity, associated  
327 to density lower than 0.5 g/cm<sup>3</sup> (Table 2) are typical of aerogels (Fricke & Tillotson, 1997).  
328 Based on these data, the sample obtained by supercritical-CO<sub>2</sub>-drying of salad waste leaves can  
329 be regarded as a bioaerogel-like material.

### 330 3.3 *Interaction of supercritical-CO<sub>2</sub>-dried salad waste with solvents*

331 The large specific surface area of bioaerogels can be exploited for sorption of bioactives and  
332 has been proposed for controlled release in pharmaceutical, food applications and innovative  
333 active food packaging. The sorption isotherm of the bioaerogel-like material obtained from  
334 salad waste was assessed to obtain preliminary information about the possibility of the material

335 to interact with hydrophilic volatiles (Figure 2). It must be noted that BET model is known to  
336 be valid for low  $a_w$  values, as well appreciable in Figure 2 (van den Berg, 1985). Regression  
337 analysis in the  $a_w$  range 0.05-0.43 provided good model fitting to data ( $R^2=0.999$ ;  $p<0.05$ ). The  
338 isotherm shape revealed the presence of a type III isotherm. This is typical of materials able to  
339 only weakly interact with water, leading to a strong increase in  $a_w$  values upon a reduced  
340 moisture increase (Figure 2). In particular, the material obtained by supercritical-CO<sub>2</sub>-drying  
341 of salad waste is expected to mainly interact with water through capillarity phenomena in its  
342 porous structure as well as through surface interactions with the hydrophilic residues present  
343 on cellulosic fibers, which are the main constituents of vegetable cell walls (Al-Muhtaseb,  
344 McMinn, & Magee, 2002; Brunauer, Deming, Deming, & Teller, 1940). Given the limited  
345 capacity to interact with water vapor, the material obtained by submitting salad waste to  
346 supercritical-CO<sub>2</sub>-drying would be physically stable under a wide range of humidity values  
347 (Figure 2). This property suggests a possible exploitation of this material for different  
348 applications, including biodegradable and edible packaging.

349 To better characterize material interactions with water vapor, its hygroscopicity was evaluated  
350 by moisture sorption kinetics (Supplementary Figure C). Moisture sorption evolved rapidly and  
351 reached a final value of about 30% within the first 20 h. This can be related to the inherent  
352 hygroscopicity of the material, rich in hydrophilic residues (Ahmadi et al., 2016), as confirmed  
353 by the FTIR spectra of the material (Supplementary Figure D). In particular, the broad band in  
354 the IR region from 3700-3000  $\text{cm}^{-1}$  and the peak at 667  $\text{cm}^{-1}$  have been associated to OH-  
355 stretching vibrations arising from hydrogen bonding and to OH out-of plane bending,  
356 respectively (Abid, Cabrales, & Haigler, 2014).

357 As reported for bioareogels, the high porosity of supercritical-CO<sub>2</sub>-dried salad waste could be  
358 exploited to entrap huge amounts of different solvents (Ahmadi et al., 2016; Manzocco et al.,  
359 2017). The capacity of supercritical-CO<sub>2</sub>-dried sample to load water and oil was thus evaluated  
360 by immersing dried leaves in the two solvents (Figure 3). Bioareogel salad waste did not lose

361 integrity upon immersion into both water and oil, taking the appearance shown in  
362 Supplementary Figure E.

363 It is noteworthy that different results were observed for other bioaerogels reported in the  
364 literature. For instance, k-carrageenan bioaerogels, although maintaining their structure upon  
365 oil immersion, quickly dissolved in water (Manzocco et al., 2017).

366 Water and oil were progressively absorbed by dried salad waste during immersion in the  
367 solvent, reaching a *plateau* value after about 40 h immersion (Figure 3). Liquid absorption by  
368 a porous material is known to be affected by different factors, such as the capacity of the  
369 material to bind the solvent (Blake, Co, & Marangoni, 2014). To further investigate these  
370 aspects, water and oil absorption kinetic of dried salad waste were fitted using a two-phase  
371 exponential decay model (TPE) (eq. 4) (Blake et al., 2014). The latter can be used to describe  
372 solvent absorption kinetics as a result of fast and slow components, which are related to the  
373 capacity of the material to bind the solvent. Data were well adapted to the model, leading to  
374 parameter estimates reported in Table 4. The TPE model used in the analysis posits that solvent  
375 absorption in the material obtained by supercritical-CO<sub>2</sub>-drying takes place according to two  
376 different phases: the first one in which solvent is loaded relatively quickly (fast phase) and the  
377 second one in which solvent is loaded relatively slowly (slow phase), both of which can be  
378 differentiated based on the respective rate constants. The fast component refers to unbound or  
379 weakly bound (physically-entrapped) solvent while the slow component is relevant to bound  
380 solvent. The rate constant for the fast-decaying and slow-decaying components ( $k_{fast}$  and  $k_{slow}$ )  
381 resulted similar ( $p \geq 0.05$ ) for water. This indicates that water absorption was equally distributed  
382 between fast and slow components, suggesting water to be both physically entrapped and  
383 chemically bound. By contrast, in the case of oil,  $k_{fast}$  resulted much higher than  $k_{slow}$ ,  
384 confirming its uptake in the material to be mainly driven by physical interactions. Absorption  
385 data were further elaborated to evidence the amount of water and oil absorbed in the fast and  
386 slow phases. Data indicate that both  $y_{fast}$  and  $y_{slow}$  resulted higher for water than oil, indicating

387 that the material presented a higher affinity toward water than oil. Moreover, the maximum  
388 amount of absorbed water and oil ( $y_{max}$ ) was estimated. Given the different density of water and  
389 oil,  $y_{max}$  was expressed as both weight and volume absorbed by 1 g of dried sample. Results  
390 indicate that the water amount absorbed by dried salad waste was significantly higher than the  
391 oil one ( $p < 0.05$ ).

392 It can be noted that supercritical-CO<sub>2</sub>-dried salad absorbed an amount of water much higher  
393 than that originally entrapped in the fresh salad tissue. The latter presented a water content of  
394 941 g/kg, corresponding to about 16 g of water for 1 g of dry sample. The enhanced ability of  
395 the material to absorb water (Table 2) could be attributed to its peculiar structure (Figure 1).  
396 However, it could be inferred that removal of compounds soluble in ethanol or CO<sub>2</sub> could lead  
397 to the exposure of hydrophilic functional groups on the surface of the fibrous network. These  
398 features would favor capillary forces and swelling phenomena, leading to both water physical  
399 entrapment and hydration of functional groups of polysaccharides. On the contrary, oil  
400 absorption would be mainly driven by capillary forces, being hindered by the hydrophilic nature  
401 of pore surfaces (Ahmadi et al., 2016). It is noteworthy that the water and oil absorption capacity  
402 showed by dried salad waste (Table 4) are much higher than those of other bioaerogels reported  
403 in the literature. In particular, Ahmadi et al. (2016) and Manzocco et al. (2017) obtained whey  
404 protein and k-carrageenan bioaerogels characterized by a maximum oil loading capacity of  
405 circa 0.025 and 0.800 g/g respectively. These findings suggest that dried salad waste can be  
406 resembled to a cloth which can uptake large amounts of water or oil. It could be exploited as  
407 template for structuring and delivering both hydrophilic and lipophilic compounds, and thus for  
408 the preparation of innovative materials to be used as oil spills absorbers or templates for  
409 hydrogels and oleogels.

## 410 **Conclusions**

411 An expanded, brittle and highly porous material was obtained by supercritical-CO<sub>2</sub>-drying of  
412 salad waste. This material was demonstrated to absorb considerable amounts of water and oil.

413 As other organic aerogels, this dried material is made from renewable sources and is completely  
414 biodegradable. Moreover, it is based on the exploitation of an industrial discard, which is  
415 always available and cheap. Based on these considerations, bioaerogel-like materials derived  
416 from supercritical-drying of salad waste could fit typical bioaerogel applications, such as  
417 thermal insulation, biodegradable packaging development and carriers for lipophilic  
418 compounds. In addition, the low firmness of dried salad waste and its capacity to withstand  
419 water contact without losing integrity suggest further possible applications, including the use  
420 as food ingredient, moisture absorber and carrier for hydrophilic molecules. Moreover, it must  
421 be underlined that the approach here proposed could be easily applied for the valorization of  
422 food industry discards other than fruit and vegetable wastes. However, in order to assess the  
423 actual feasibility of this valorization strategy for vegetable waste, the evaluation of  
424 sustainability, economic and consumer impact of the obtained material should be carefully  
425 investigated. In particular, the high costs of supercritical-CO<sub>2</sub>-drying technology could  
426 represent a critical issue. Similarly, the perishable nature of salad waste, which is prone to  
427 microbiological spoilage in few hours, would impose a selection of salad waste to remove  
428 bruised and spoiled parts and a subsequent quick transformation into a dried material. Finally,  
429 specific approaches should be adopted to provide the bioaerogel-like material with the desired  
430 shape, making it independent on the original dimension of the used vegetable waste. To this  
431 regard, the application to the ground vegetable waste of approaches commonly used to produce  
432 hydrogel and oleogel templates could be evaluated.

433

434 This research did not receive any specific grant from funding agencies in the public,  
435 commercial, or not-for-profit sectors.

437 **References**

- 438 Abid, N., Cabrales, L., & Haigler, C. H. (2014). Changes in the cell wall and cellulose content  
439 of developing cotton fibres investigated by FTIR spectroscopy. *Carbohydrate Polymers*,  
440 *100*, 9-16.
- 441 Ahmadi, M., Madadlou, A., & Saboury, A. A. (2016). Whey protein aerogel as blended with  
442 cellulose crystalline particles or loaded with fish oil. *Food Chemistry*, *196*, 1016-1022.
- 443 Al-Muhtaseb, A. H., McMinn, W. A. M., & Magee, T. R. A. (2002). Moisture Sorption  
444 Isotherm Characteristics of Food Products: A Review. *Food and Bioproducts Processing*,  
445 *80*, 118-128.
- 446 Amin, J. S., Abkenar, M. V., & Zendehboudi, S. (2015). Natural sorbent for oil spill cleanup  
447 from water surface: Environmental implication. *Industrial & Engineering Chemical*  
448 *research*, *54*, 10615-10621.
- 449 AOAC (1997). Official methods of analysis. Washington, DC: Association of Official  
450 Analytical Chemists.
- 451 Blake, A. I., Co, E. D., & Marangoni, A. G. (2014). Structure and physical properties of plant  
452 wax crystal networks and their relationship to oil binding capacity. *Journal of the*  
453 *American Oil Chemists' Society*, *91*, 885-903.
- 454 Braunauer, S., Emmett, P. H., & Teller, E. (1938). Adsorption of gases in multimolecular layers.  
455 *Journal of the American Chemical Society*, *60*, 309-319.
- 456 Brown, Z. K., Fryer, P. J., Norton, I. T., Bakalis, S., & Bridson, R. H. (2008). Drying of foods  
457 using supercritical carbon dioxide - Investigations with carrot. *Innovative Food Science &*  
458 *Emerging Technologies*, *9*, 280-289.
- 459 Brunauer, S., Deming, L. S., Deming, W. E., & Teller, E. (1940). On a Theory of the van der  
460 Waals Adsorption of Gases. *Journal of the American Chemical Society*, *62*, 1723-1732.
- 461 Chen, Z., Zhu, C., Zhang, Y., Niu, D., & Du, J. (2010). Postharvest biology and technology  
462 effects of aqueous chlorine dioxide treatment on enzymatic browning and shelf-life of

463 fresh-cut asparagus lettuce (*Lactuca sativa* L.). *Postharvest Biology and Technology*, 58,  
464 232-238.

465 Comin, L. M., Temelli, F., & Saldaña, M. D. A. (2012). Barley  $\beta$ -glucan aerogels as a carrier  
466 for flax oil via supercritical CO<sub>2</sub>. *Journal of Food Engineering*, 111(4), 625-631.

467 Fiori, L., de Faveri, D., Casazza, A. A., & Perego, P. (2009). Grape by-products: extraction of  
468 polyphenolic compounds using supercritical CO<sub>2</sub> and liquid organic solvent-a preliminary  
469 investigation. *CyTA-Journal of Food*, 7, 163-171.

470 Fricke, J., & Tillotson, T. (1997). Aerogels: production, characterization, and applications. *Thin*  
471 *Solid Films*, 297, 212-223.

472 García-González, C. A., Camino-Rey, M. C., Alnaief, M., Zetzl, C., & Smirnova, I. (2012).  
473 Supercritical drying of aerogels using CO<sub>2</sub>: Effect of extraction time on the end material  
474 textural properties. *The Journal of Supercritical Fluids*, 66, 297-306.

475 Ghafar, A., Gurikov, P., Subrahmanyam, R., Parikka, K., Tenkanen, M., Smirnova, I., &  
476 Mikkonen, K. S. (2017). Mesoporous guar galactomannan based biocomposite aerogels  
477 through enzymatic crosslinking. *Composites Part A*, 94, 93-103.

478 Guedes, A. C., Gião, M. S., Matias, A. A., Nunes, A. V. M., Pintado, M. E., Duarte, C. M. M.,  
479 & Malcata, F. X. (2013). Supercritical fluid extraction of carotenoids and chlorophylls a,  
480 b and c, from a wild strain of *Scenedesmus obliquus* for use in food processing. *Journal*  
481 *of Food Engineering*, 116, 478-482.

482 Ivanovic, J., Milovanovic, S., & Zizovic, I. (2016). Utilization of supercritical CO<sub>2</sub> as a  
483 processing aid in setting functionality of starch-based materials. *Starch - Stärke*, 68, 821-  
484 833.

485 Khosravi, M., & Azizian, S. (2016). A new kinetic model for absorption of oil spill by porous  
486 materials. *Microporous and Mesoporous Materials*, 230, 25-29.

487 Krokida, M. K., Maroulis, Z. B., & Saravacos, G. D. (2001). The effect of the method of drying  
488 on the colour of dehydrated products. *International Journal of Food Science and*

- 489        *Technology*, 36, 53-59.
- 490        Lan, S., Wu, L., Zhang, D., Hu, C., & Liu, Y. (2011). Ethanol outperforms multiple solvents in  
491        the extraction of chlorophyll-a from biological soil crusts. *Soil Biology and Biochemistry*,  
492        43, 857–861.
- 493        Lichtenthaler, H. K., & Buschmann, C. (2001). Chlorophylls and carotenoids: Measurement  
494        and characterization by UV-VIS spectroscopy. *Current Protocols in Food Analytical*  
495        *Chemistry*, F4:3.1-F4:3.8.
- 496        Maleki, H. (2016). Recent advances in aerogels for environmental remediation applications: A  
497        review. *Chemical Engineering Journal*, 300, 98-118.
- 498        Manzocco, L., Valoppi, F., Calligaris, S., Andreatta, F., Spilimbergo, S., & Cristina, M. (2017).  
499        Exploitation of k -carrageenan aerogels as template for edible oleogel preparation. *Food*  
500        *Hydrocolloids*, 71, 68-75.
- 501        Michalska, A., Wojdyło, A., Lech, K., Łysiak, G. P., & Figiel, A. (2017). Effect of different  
502        drying techniques on physical properties, total polyphenols and antioxidant capacity of  
503        blackcurrant pomace powders. *LWT - Food Science and Technology*, 78, 114-121.
- 504        Mykhailiyk, V., & Lebovka, N. I. (2013). Specific heat of apple at different moisture contents  
505        and temperatures. *Journal of Food Engineering*, 123, 32-35.
- 506        Plazzotta, S., Manzocco, L., & Nicoli, M. C. (2017). Fruit and vegetable waste management and  
507        the challenge of fresh-cut salad. *Trends in Food Science & Technology*, 63, 51-59.
- 508        Perucka, I., Olszówka, K. & Chilczuk, B. (2014). Changes in the chlorophyll content in stored  
509        lettuce *Lactuca sativa* L. after pre-harvest foliar application of CaCl<sub>2</sub>. *Acta Agrobotanica*,  
510        66, 137-142.
- 511        Raak, N., Symmank, C., Zahn, S., Aschemann-Witzel, J., & Rohm, H. (2017). Processing- and  
512        product-related causes for food waste and implications for the food supply chain. *Waste*  
513        *Management*, 61, 461-472.
- 514        Roy, B. C., Goto, M., Kodama, A., & Hirose, T. (1996). Supercritical CO<sub>2</sub> extraction of



515 essential oils and cuticular waxes from peppermint leaves. *Journal of Chemical*  
516 *Technology & Biotechnology*, 67, 21–26.

517 Singleton, V. L., & Rossi, J. A. J. (1985). Colorimetry of total phenolics with phosphomolybdic-  
518 phosphotungstic acid reagents. *American Journal of Enology and Viticulture*, 16, 144–  
519 158.

520 Stergar, J., & Maver, U. (2016). Review of aerogel-based materials in biomedical applications.  
521 *Journal of Sol-Gel Science and Technology*, 77, 738-752.

522 Su, J. F., Huang, Z., Zhao, Y. H., Yuan, X. Y., Wang, X. Y., & Li, M. (2010). Moisture sorption  
523 and water vapor permeability of soy protein isolate/poly (vinylalcohol)/glycerol blend  
524 films. *Industrial Crops and Products*, 31, 266-276.

525 Therkelsen, G. H. (1993). Carrageenan. In R. L. Whistler, & J. N. BeMiller (Eds.), *Industrial*  
526 *Gums: Polysaccharides and their derivatives* (Third ed., pp. 146e176). San Diego (USA):  
527 Academic Press, Inc.

528 Ubeyitogullari, A., & Ciftci, O. N. (2017). Generating phytosterol nanoparticles in nanoporous  
529 bioaerogels via supercritical carbon dioxide impregnation: Effect of impregnation  
530 conditions. *Journal of Food Engineering*, 207, 99-107.

531 van den Berg, C. (1985). “Development of B.E.T.-like models for sorption of water on foods,  
532 theory and relevance”. In *Properties of water in foods: in relation to quality and stability*,  
533 edited by D. Simatos and J L Multon, 119-131. Nato ASI Series: Springer.

534 Viganó, J., Machado, A. P. da F., & Martínez, J. (2015). Sub- and supercritical fluid technology  
535 applied to food waste processing. *The Journal of Supercritical Fluids*, 96, 272-286.

536 Wiman, M., Dienes, D., Hansen, M. A. T. van der Meulen, T., Lidén, G., & Zacchi, G. (2012).  
537 Cellulose accessibility determines the rate of enzymatic hydrolysis of steam-pretreated  
538 spruce. *Bioresource Technology*, 126, 208-215.

539

541 **Figure Captions**

542 Figure 1. Visual appearance, color and microscopic images of fresh salad leaves and salad  
543 leaves dried using supercritical CO<sub>2</sub>.

544 Figure 2. Isotherm of supercritical-CO<sub>2</sub>-dried salad waste. Fitting curve of BET model (BET)  
545 to experimental data (Data) is also reported. ds =dry sample.

546 Figure 3. Absorption of water and oil by supercritical-CO<sub>2</sub>-dried salad waste. Fitting curves of  
547 the two-phase exponential model (TPE) are also reported. ds =dry sample.

548

549 **Supplementary Figure Captions**

550 Supplementary Figure A. Stress-strain diagram of supercritical-CO<sub>2</sub>-dried salad waste.

551 Supplementary Figure B. Nitrogen adsorption (ads) and desorption (des) isotherms of  
552 supercritical-CO<sub>2</sub>-dried salad waste.

553 Supplementary Figure C. Moisture sorption (MS) versus time diagram of the supercritical-  
554 CO<sub>2</sub>-dried salad waste.

555 Supplementary Figure D. FTIR spectra of supercritical-CO<sub>2</sub>-dried salad waste. AU =  
556 absorbance unit

557 Supplementary Figure E. Visual appearance of supercritical-CO<sub>2</sub>-dried salad waste after  
558 immersion in water.

560 Table 1. Composition of salad waste.

	Amount in fresh salad (g/kg)
Humidity	945 ± 6
Carbohydrates	28.8 ± 0.6
Total dietary fibre	13.3 ± 0.2
Proteins	10.5 ± 0.8
Ash	2.55 ± 0.11
Fat	2.05 ± 0.07
Total polyphenols (GAE)	0.0722 ± 0.0055
Chlorophylls	0.00765 ± 0.00013

561

562

563

564 Table 2. Specific heat capacity, mechanical properties (tensile strength and elongation at

565 break), apparent density and specific volume of supercritical-CO<sub>2</sub>-dried salad waste.

Specific heat capacity (Jg <sup>-1</sup> K <sup>-1</sup> )	Tensile strength at break (N)	Elongation at break (mm)	Apparent density (g/cm <sup>3</sup> )	Specific volume (cm <sup>3</sup> /g)
2.617 ± 0.034	0.18 ± 0.10	0.21 ± 0.05	0.032 ± 0.004	31.3 ± 3.4

566

567

568 Table 3. Characteristics of mesopores, macropores, and total porosity of supercritical-CO<sub>2</sub>-  
 569 dried salad leaves.

Mesopores <sup>a</sup>				Macropores			Total pores <sup>d</sup>	
Surface area (m <sup>2</sup> /g)	Total pore volume (cm <sup>3</sup> /g)	Pore dimension (nm)	Total pore volume ratio (%)	Total pore volume <sup>c</sup> (cm <sup>3</sup> /g)	Pore dimension <sup>b</sup> (μm)	Total pore volume ratio <sup>c</sup> (%)	Total pore volume (cm <sup>3</sup> /g)	Total porosity (%)
112.8 ± 8.2	2.80 ± 0.30	46.8 ± 1.9	10.9 ± 0.2	22.8 ± 0.4	111.1 ± 35.3	89.1 ± 1.6	25.6 ± 0.4	81.7 ± 1.4

570 <sup>a</sup> estimated by BET technique

571 <sup>b</sup> estimated by image analysis of photomicrographs

572 <sup>c</sup> estimated by difference between data of total pores and mesopores

573 <sup>d</sup> estimated by oil imbibition


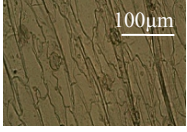

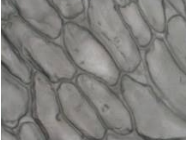
574

575

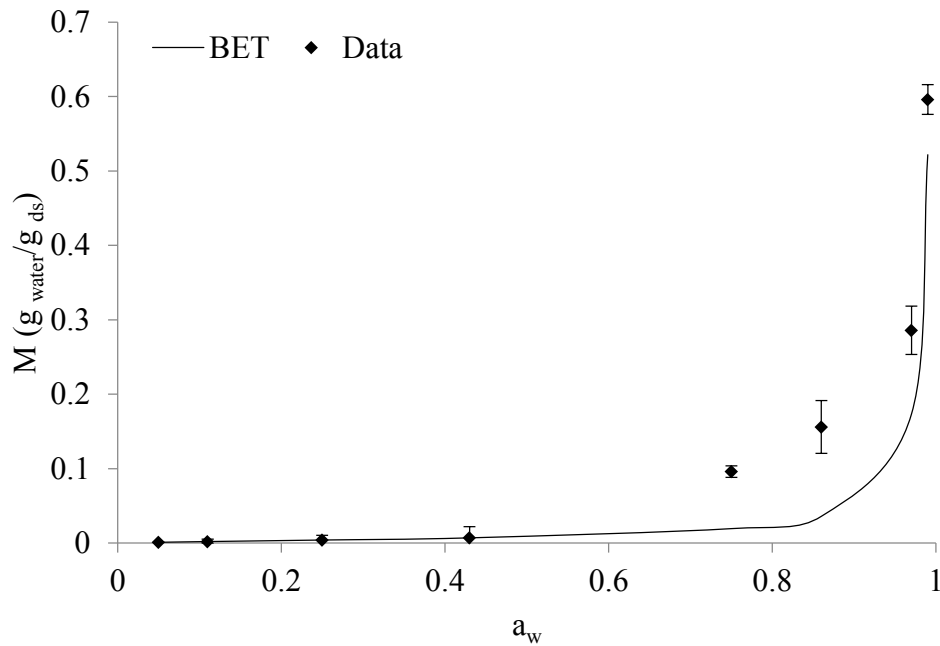
576 Table 4. Experimental regression coefficients estimate, R<sup>2</sup> and adjusted R<sup>2</sup> for the two-phase  
 577 exponential model (TPE) and for the solvent spill absorption model (SSA) of water and oil  
 578 absorption in supercritical-CO<sub>2</sub>-dried salad waste. Water and oil absorption capacity is also  
 579 reported.

	Water	Oil
$k_{fast}$ (h <sup>-1</sup> )	0.431 ± 0.013	248.2 ± 13.6
$k_{slow}$ (h <sup>-1</sup> )	0.465 ± 0.016	0.175 ± 0.007
$y_{fast}$ (g solvent/g ds)	16.8 ± 0.8	10.6 ± 0.2
$y_{slow}$ (g solvent/g ds)	16.8 ± 0.9	8.5 ± 0.4
$y_{max}$ (g solvent/g ds)	33.5 ± 1.4	19.1 ± 1.3
$y_{max}$ (mL solvent/g ds)	37.6 ± 1.6	21.4 ± 1.5
R <sup>2</sup>	0.944	0.967
R <sup>2</sup> adj	0.929	0.954
Absorption capacity (g/g)	0.97 ± 0.02	0.95 ± 0.02

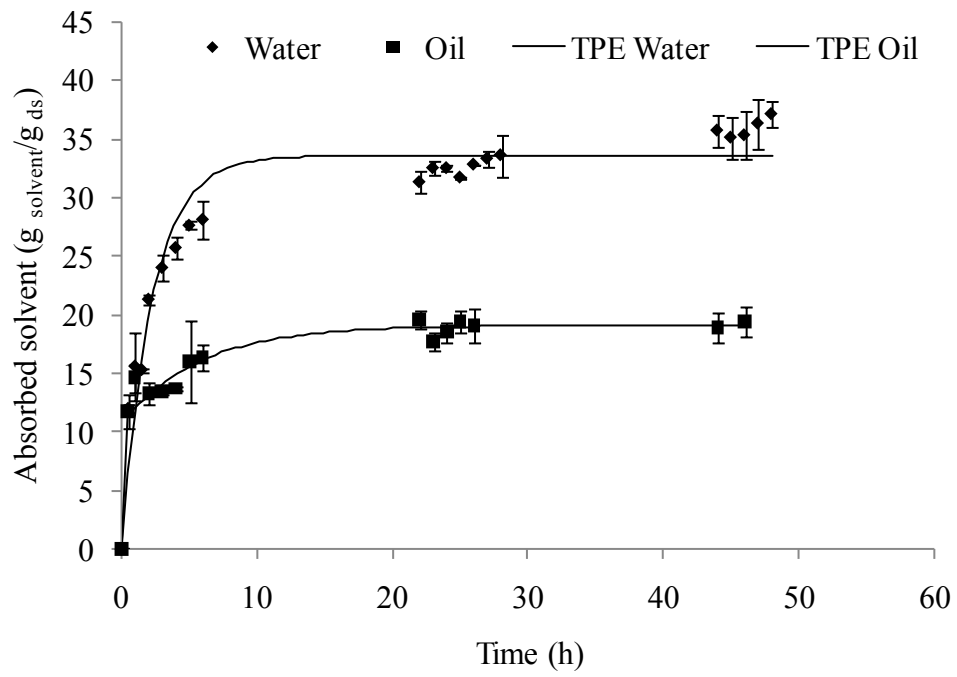
580

Sample	Visual appearance	Color			Optical microscopy
		L*	a*	b*	
Fresh		71.4 ± 1.3	-16.9 ± 1.2	31.6 ± 1.4	
Dried		85.0 ± 2.4	-0.2 ± 0.1	8.7 ± 0.4	

1 Figure 1. Visual appearance, color and microscopic images of fresh salad leaves and salad  
2 leaves dried using supercritical CO<sub>2</sub>.



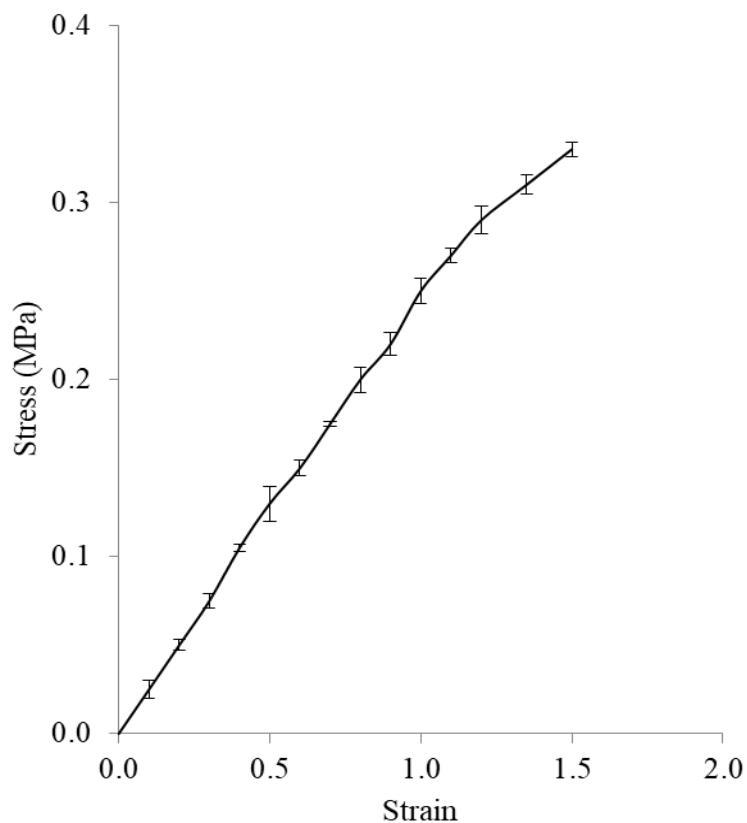
8  
9 Figure 2. Isotherm of supercritical-CO<sub>2</sub>-dried salad waste. Fitting curve of BET model (BET)  
10 to experimental data (Data) is also reported. ds =dry sample.



12  
13  
14  
15

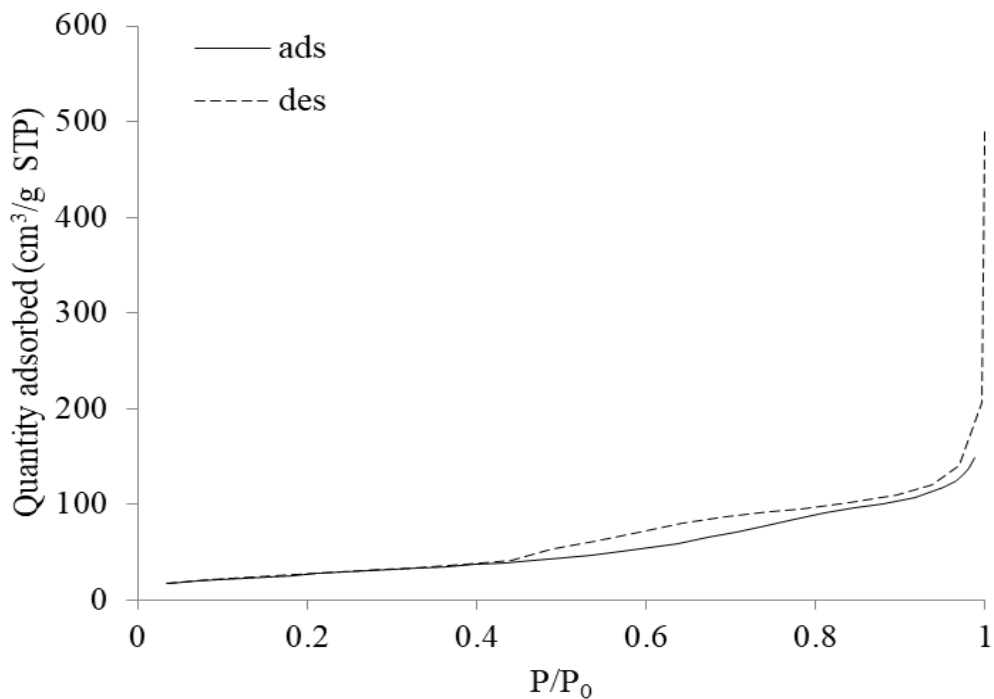
Figure 3. Absorption of water and oil by supercritical-CO<sub>2</sub>-dried salad waste. Fitting curves of the two-phase exponential model (TPE) are also reported. ds =dry sample.

1 **Supplementary data**



2  
3 **Supplementary Figure A. Stress-strain diagram of supercritical-CO<sub>2</sub>-dried salad waste.**

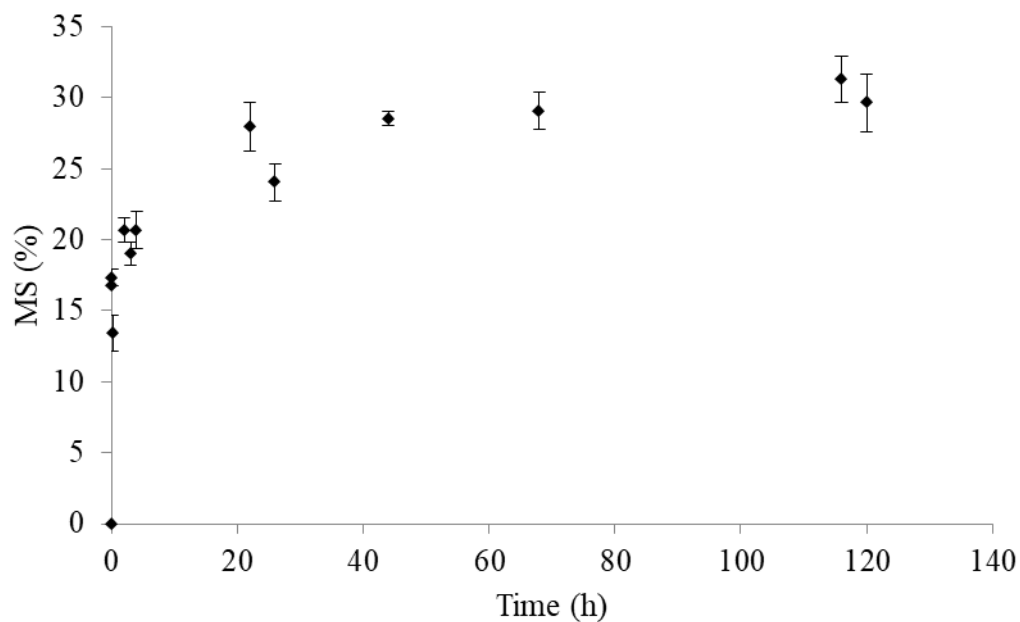
4  
5



6  
7 **Supplementary Figure B. Nitrogen adsorption (ads) and desorption (des) isotherms of**  
8 **supercritical-CO<sub>2</sub>-dried salad waste.**

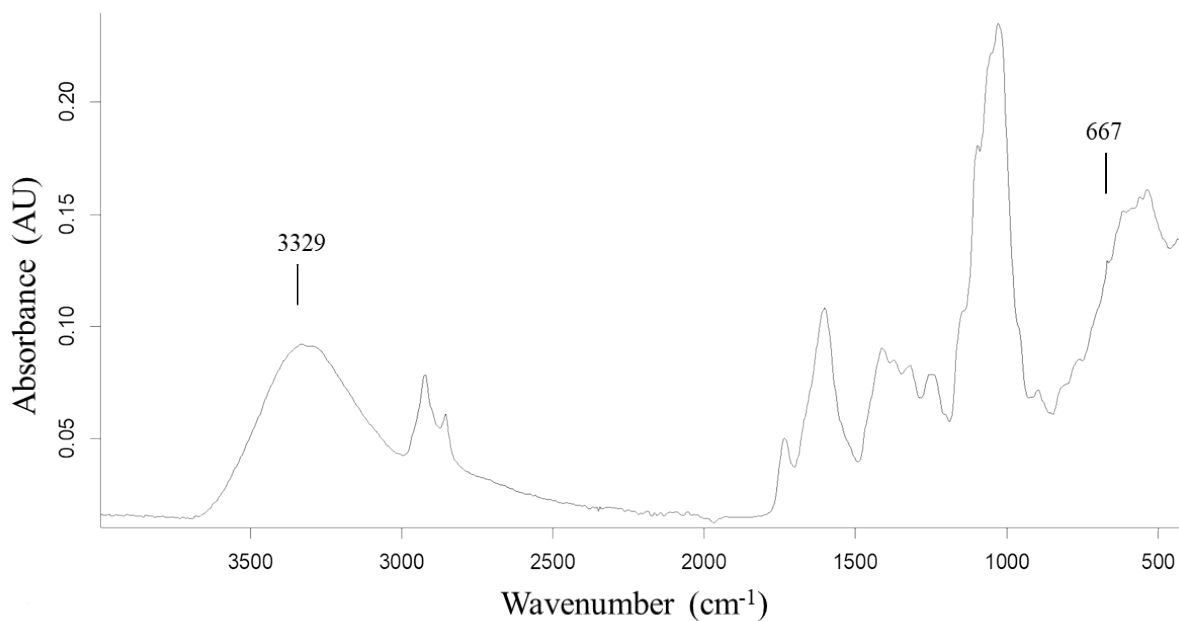
9  
10

11



12  
13  
14  
15  
16  
17

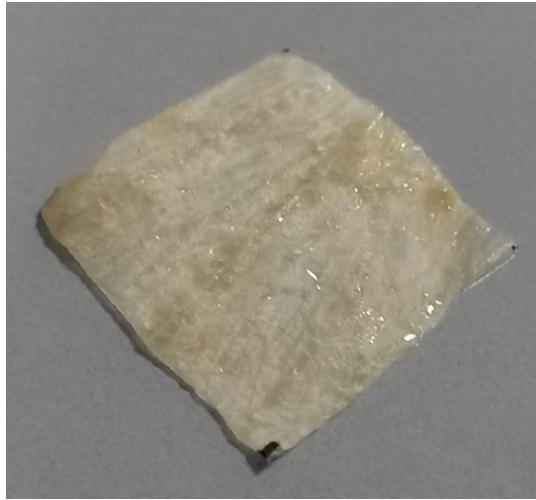
Supplementary Figure C. Moisture sorption (MS) versus time diagram of the supercritical-CO<sub>2</sub>-dried salad waste.



18  
19  
20  
21

Supplementary Figure D. FTIR spectra of supercritical-CO<sub>2</sub>-dried salad waste. AU = absorbance unit





22  
23  
24

Supplementary Figure E. Visual appearance of supercritical-CO<sub>2</sub>-dried salad waste after immersion in water.